DOI: 10.31401/WS.2021.proc.39

Criteria for identification of geoeffective solar events

Georgieva K., Asenovski S., Kirov B.

SRTI-BAS; kgeorgieva@space.bas.bg

1. Abstract

"Space weather" is defined as conditions in the interplanetary and near-Earth space that can affect the performance and reliability of space-borne and ground-based technology, as well as human life and physiological conditions. It is well known that the drivers of space weather are geoeffective solar transients propagating from the Sun to the Earth. These drivers have different characteristics and different effects on the Earth. Various authors have proposed different criteria to identify these solar activity drivers. After a brief overview of the proposed so far criteria, we formulate our own criteria to be used for identifying geoeffective solar drivers and their effects on space weather.

Keywords: space weather, geoeffective solar agents, criteria

2. Introduction

There are basically three types of solar wind in which the Earth is immersed: slow solar wind (SSW) from the streamer belt, high speed solar wind streams (HSS) from solar coronal holes, and coronal mass ejections (CMEs).

The physical mechanism for the coupling of the interplanetary magnetic field (IMF) with the Earth's magnetic field is magnetic reconnection which is possible when the IMF vertical component Bz is negative – southward (Dungey, …). The energy transfer from the solar wind to the magnetosphere is different for CMEs and HSS (Tsurutani and Gonzalez, 1997) and, consequently, the geomagnetic disturbances which they cause are also different.

If a CME is faster than the ambient solar wind, it drives a shock/sheath ahead of it and the storm has an initial phase caused by the increase in the plasma ram pressure associated with the increase in density and speed in the sheath at the interface between the CME and the Earth's magnetosphere. The storm's main phase is due to the southward IMFs in the ejecta itself. If the fields are southward in both of the sheath and the ejecta, a two-step main phase storm can result. The storm recovery phase begins when the IMF turns less southward, and lasts for about 10 hours (Tsurutani and Gonzalez, 1997).

Corotating Interaction Regions (CIRs) are created when fast HSS emanating from the solar coronal holes interact with the high density, low-speed solar wind associated with the heliospheric current sheet. As the Bz component in CIRs is typically highly fluctuating, the main phases of the resultant magnetic storms typically have highly irregular profiles and are weaker than the ones caused by CMEs. On the other hand, the CIR-related storm recovery phases can last from many days to weeks (Tsurutani and Gonzalez, 1997). Therefore, though the most intense geomagnetic storms (defined by Kp) at both solar minimum and solar maximum are almost all generated by CMEs, the long-term (> solar rotation) averages of the geomagnetic activity indices closely follow the magnetic field variations in CIRs and slow solar wind (Richardson et al., 2002).

3. Identification schemes

3.1. Previous classifications

The **coronal mass ejections** originate from active regions of closed field lines, so their number and intensity are related to the number and surface area of sunspots which are also associated with regions of closed field lines. When enough energy is accumulated so that the such an active region loses stability, it ejects coronal matter with embedded magnetic fields. CMEs are characterized by unusually low proton temperature or low plasma beta (ratio of plasma pressure to magnetic pressure), composition anomalies, bidirectional suprathermal electron strahls indicating looped magnetic field lines rooted at both ends on the Sun. Fast CME's drive shocks with enhanced plasma speed, density and temperature. An Earth-directed CME is observed as a halo around the Sun. A subclass of CME's are magnetic clouds (MC's) distinguished by enhanced magnetic field with smooth rotation inside the structure.

Various methodologies have been developed to identify and separate CMEs and magnetic clouds. The earlier ones mainly focused on anomalously low proton temperatures (Gosling et al., 1973; Elliott et al., 2005). Gosling et al. (1987) and Skoug et al. (2000) looked for the presence of a bidirectional electron strahl indicating that both ends of the magnetic field tube are attached to the solar surface. Cane and Richardson (2003) and Richardson and Cane (2010) provided a list of CMEs in the near-Earth space based on the combination of proton temperature, O7+/O6+ density ratio, electron strahl, magnetic field structure, and energetic particle measurements. An important parameter is the ration between the observed and expected proton velocity Tp/Texp, where Texp is the expected temperature for the observed solar wind speed Vsw:

T_{ex}= 3(0.0106V_{sw} – 0.287) if V_{sw} < 500 km/s and

T_{ex} = (0.77V_{sw} – 265) if V_{sw} > 500 km/s

In this list, Cane and Richardson 2003) included all CMEs, both magnetic cloud and mon-magnetic cloud ones. On the other hand, Lepping et al. (2005), Wu et al. (2011) compiled lists of only magnetic clouds. To this end, they developed a computer program to automatically detect MCs and MC-like structures, based on requirements for 1) enhanced magnetic field strength, 2) a smooth change in field direction as observed by a spacecraft passing through the MC, and 3) low proton temperature (and low proton plasma beta) compared to the ambient plasma. Jian et al. (2006) produced a catalog of ICMEs at Earth based on the total pressure, the proton temperature, the alpha-to-proton density ratio, the magnetic field structure, and the presence of bidirectional electron streaming.

We are here concentrating on criteria which can be calculated from data included in OMNI and OMNI2 database because they cover the longest period of in situ measurements.

Yermolaev et al. (2009) formulated 9 solar wind types, and used a preliminary identification program with preset threshold criteria for the plasma types to identify them based on parameters calculated from data compiled in the original OMNI database (for more details, see their Table 1):

1) Heliospheric current sheet: N<7 cm^{-3}; V<500 km/s; β>0.7
2) Slow solar wind: N>3 cm^{-3}; V<450 km/s; β<1
3) Fast solar wind: N<20 cm^{-3}; V≥450 km/s; β<1
4) Corotation interaction region: N>3 cm^{-3}; B>5 nT; T/T_{exp}>1; thermal pressure NkT >0.007; β<1
5) Ejecta (CMEs): N<10; T/Texp<0.5; NkT<0.01; β<0.5
6) Magnetic clouds: N<10; B>10; T/Texp<0.5; NkT<0.01; β<0.5
7) Rarefaction regions: N ≤1; V <500; T/Texp<1; NkT<0.01.

We are not dealing here with the IS - forward interplanetary shock, and ISa - reverse interplanetary shock, as these events are very short, of the order of a minute.

Xu and Borovsky (2014) defined 4 categories of geoeffective solar transients, further separating the slow solar wind into streamer belt solar wind plasma and sector-reversal-region plasma. The authors used the Lepping et al. (2005) list of MCs, with the continuation by Wu et al. (2011). They conducted a detailed study of the separation of the 4 categories, and presented criteria for separating MCs from the other geoeffective drivers. Fig.1, upper left, demonstrates that MCs are easily distinguishable from other solar wind transients in terms of plasma beta. MCs (ejecta) have much lower plasma beta than HSS-related ("coronal hole") and slow solar wind ("streamer belt" and "sector reversal region" plasma). This is confirmed by Fig.1, upper right, illustrating the ratio between the expected and the observed proton temperature in the different solar wind structures. This ratio is much higher in CME ("ejecta") type plasma than in all other transients. Another indicative parameter is the Alfven speed which in the case of CMEs is lower than the other categories (Fig.1, bottom right). Finally, Fig.1, bottom left demonstrates that the magnetic field fluctuations in a MC (and in a CME in general) are much lower than in other solar wind times.

Based on these statistical results, Xu and Borovsky (2014) developed an algebraic scheme to categorize the solar wind plasma into the above four types. The scheme uses three solar wind parameters: (1) the proton-specific entropy $S_p = T_p/n_p^{2/3}$, (2) the proton Alfvén speed $V_A = B/(4\pi m_p n_p)^{1/2}$, and (3) the ratio of the measured proton temperature T_p compared with the velocity-dependent expected temperature for the solar wind speed $T_{exp} = (V_{sw}/258)^{3.113}$. To calculate those three parameters, four solar wind quantities are used: the proton number density n_p, the proton temperature T_p, the magnetic field strength B, and the solar wind speed V_{sw}.

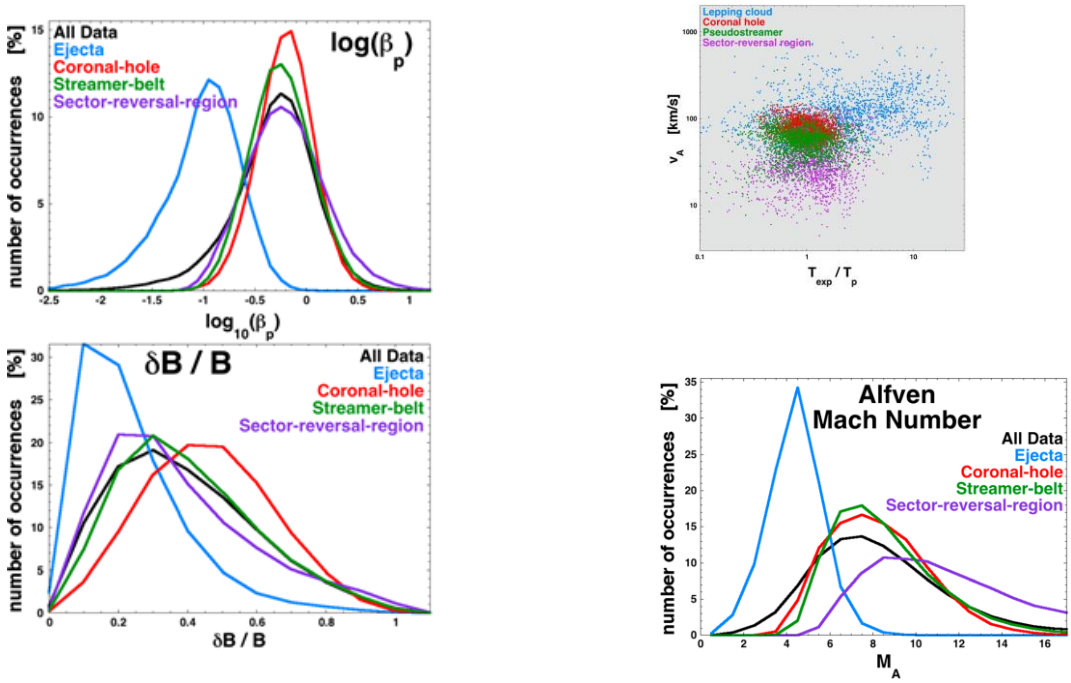

Figure1. Comparison of MC, HSS, streamer belt and sector reversal region plasma (see the text). From Xu and Borovsky (2014).

Veselovsky et al. (2018) produced a binary classification of solar wind types according to three main hydrodynamic parameters—the proton speed, the proton temperature, and the proton density, and therefore 9 types of solar wind types which arise at different frequencies and originate from different sorts of solar activity:

(1) fast–hot–dense, (2) fast–hot–rarefied, (3) fast–cold–dense, (4) fast–cold–rarefied,
(5) slow–hot–dense, (6) slow–hot–rarefied, (7) slow–cold–dense, (8) slow–cold–rarefied.
They assumed that a solar wind is:

fast if V >450 km/s and slow if V <400 km/s; hot if $T > 10^5$ K and cold if $T < 7.5 \times 10^4$ K,
dense if $n > 6$ cm^{-3} and rarefied if $n < 5$ cm^{-3}.

If at least one parameter turns to be within the excluded interval, the respective wind is categorized as (9) – "zero type" which is found to cover about 32.5% of time. The second most frequent type of solar wind (25.2%) is ***fhr*** which originates from long-term flows from coronal holes, and the third one is ***scd*** which is formed by flows from coronal streamers and pseudostreamers, as well as by heliospheric plasma layers near magnetic sectors.

Feldman et al. (1976) studied the high-speed solar wind flow parameters at 1 AU, and accepted a stream for study only if the maximum speed exceeded 650 km/s. According to Bame et al. (1976), an HSS is an observed variation of solar wind speed, with an increase of at least 150 km/s within a five-day interval during which the speed stays above $(V_0 + V_m)/2$ where V_0 is the base speed out of which the stream rises, and V_m is the maximum speed attained within the stream.

Broussard et al. (1978) defined it as a period in which the solar wind speed is faster than 500 km/s averaged over a day.

Venkatesan et al. (1982) defined the starting day of a high speed stream by a substantial increase ($\Delta V \gtrsim 200$ km/s) in the solar wind speed to values of $\gtrsim 550$ km/s and which persists at such high values for an interval of at least three days.

Lindblad and Lundstedt (1981) provided a **catalogue** of high speed solar wind streams during 1964-75. In this period, 346 streams were detected, defined as periods in which the velocity difference between the lowest 3-h velocity value and the highest 3-h value of the following day is greater than 100 km/s, and it lasts for at least two days. Two continuations of this catalogue were published: for the period 1975-78 (Lindblad and Lundstedt, 1983), and for the period 1978-82 (Lindblad et al., 1989).

Mavromichalaki et al. (1988) and Mavromichalaki and Vassilaki (1998) updated the catalogues of Lindblad and Lundstedt, using the same criteria as Lindblad and Lundstedt (1981). Additionally, Mavromichalaki et al. (1988) divided the high speed solar wind streams into two groups: ones originating from coronal holes ("Corotating Streams"), and others related to active regions ("Flare Generated Streams"). The authors showed that the magnetic field magnitude and polarity, bulk speed, proton density, and temperature of the solar wind are different for the two types of streams. Maris and Maris (2005) further extended and derailed this group of catalogs, adding the parameter "importance" I and "sum importance" ΣI of the stream $I = \Delta V_{max} * d$ where $\Delta V_{max} = (V_{max} - V_0)$, d is the duration of the high speed stream, V_{max} is its maximum daily mean velocity, and V_0 is the mean velocity.

3.2. Our classification

3.2.1. CMEs

Comparing the various catalogs, it can be noted that they do not always coincide.
As an example, we look at the most powerful CME of 2011, Dst=-147 (Fig.1).

- Cane and Richardson have determined that the CME started at 22:00 on October 24 and ended at 16:00 on October 25;
- In Xu and Borovsky's list the CME started at 23:00 on October 24 and ended at 21:00 on October 25;
- In Yermolaev et al's list this CME has been identified as a magnetic cloud lasting from 12:00 on October 23 to 12:00 on October 24.

One of the reasons for the discrepancies lies in the different definitions of the expected proton temperature based on the solar wind velocity (see above). We have performed visual inspection of the CMEs included in the various catalogs, and have formulated the following criteria for identifying a CME:

-Proton temperature $Tp < 0.5T\text{exp}$, where $T\text{exp} = 3(0.0106V\text{sw} - 0.287)$ if $V\text{sw} < 500$ km/s and $T\text{exp} = (0.77V\text{sw} - 265)$ if $V\text{sw} > 500$ km/s

-Magnetic field magnitude $B \geq 10$ nT

-Plasma Beta ≤ 0.8 for at least 5 hours.

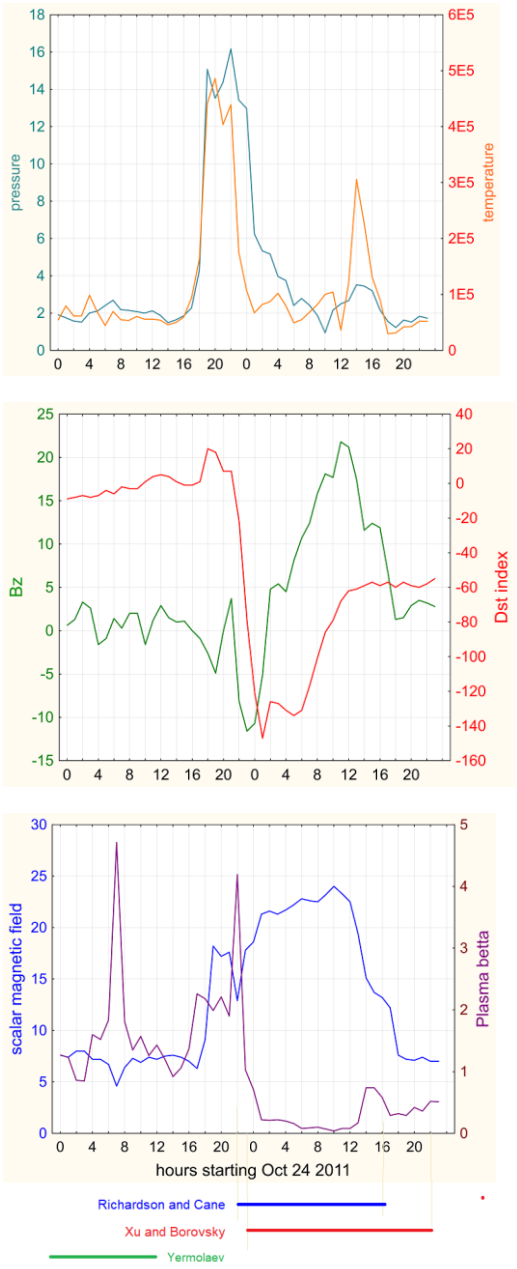

Fig.2 (left). Parameters of a CME observed in October 2011 (first 3 panels) together with its duration determined in the catalogs of Richardson and Cane (blue horizontal line), Xu and Borovsky (red horizontal line) and of Yermolaev (green horizontal line)

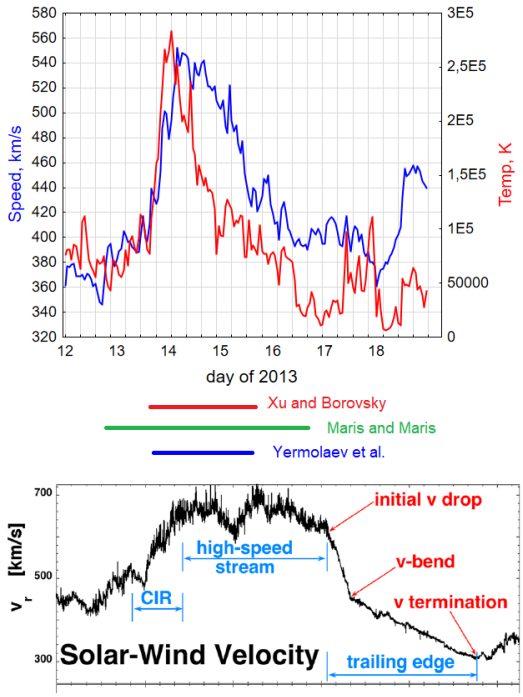

Fig.3 (upper panel) A HSS in January 2013 with its duration determined in the catalogs of Xu and Borovsky (red horizontal line) Maris and Maris (green horizontal line)and of Yermolaev (blue horizontal line); Bottom panel: the definition of the phases of a HSS by Borovsky and Denton (2016).

3.2.2. HSS

Fig.3 presents a HSS in January 2013. In Xu and Borovsky's list this HSS starts at 21:00 on January 13 and ends on 13:00 on January 15. In the catalog of Maris and Maris it starts between 15:00 and 19:00 on January 12 and ends between 19:00 and 21:00 on January 16. In Yermolaev's catalog the fast wind starts at 18:00 on January 13 and lasts until 12:00 on January 15.

The main difference is the determination of the end of the HSS. We have adopted the definition of Borovsky and Denton (2016) presented in the bottom panel of Fig.3. According to it, a HSS starts with a corotating interaction region (CIR) characterized by a sharp jump in the plasma speed, density and temperature, followed by the body co high speed stream with persisting high plasma flow speed, then by a two-step decrease of the speed, and ends with the beginning of the velocity rise.

Our criteria for a HSS include an increase of the solar wind velocity by at least 100 km/s in no more than one day to at least 500 km/s for at least 5 hours, accompanied by high temperature ($T_p > T_{exp}$) and low density, and lasts until V increase for at least 5 hours.

Acknowledgements

This research has been supported by the National Science Fund grant KP-06-N44/2.

References

Bame, S.J., Asbridg,e J.R., Feldman, W.C., Gosling, J. (1976) Solar cycle evolution of high-speed solar wind streams. Astrophysical Journal 207, Aug. 1, 1976, pt. 1, p. 977-980, doi:10.1086/154566

Borovsky, J.E., Denton, M.H. (2016) The trailing edges of high-speed streams at 1 AU. JGR Space Physics 121 (7), 107-6140, https://doi.org/10.1002/2016JA022863

Broussard, R.M., Sheeley, N.R. Jr., Tousey, R., Underwood, J. H., (1978) A survey of coronal holes and their solar wind associations throughout sunspot cycle 20. Solar Physics 56 (1), 161-183, DOI:10.1007/BF00152641,

Cane H.V., and I. G. Richardson (2003), Interplanetary coronal mass ejections in the near-Earth solar wind during 1996–2002, J. Geophys. Res., 108, 1156, doi:10.1029/2002JA009817.

Elliott, H.A., D.J. McComas, N.A. Schwadron, J. T. Gosling, R.M. Skoug, G. Gloeckler, and T. H. Zurbuchen (2005), An improved expected temperature formula for identifying ICMEs, J. Geophys. Res., 110, A04103, doi:10.1029/2004JA010794.

Farrell, W.M., Desch, M.D. (2002). Solar proton events and the fair weather electric field at ground, Geophys. Res. Lett., Vol 29, No 9, pp. 1323- 1326, DOI: 10.1029/2001GL013908.

Feldman W.C., Asbridge J.R., Bame S.J. Gosling J.T. (1076) High-speed solar wind flow parameters at 1 AU. Journal of Geophysical Research, Volume 81, Issue A28, p. 5054-5061, DOI:10.1029/JA081i028p05054.

Gosling, J. T., V. Pizzo, and S. J. Bame (1973), Anomalously low proton temperatures in the solar wind following interplanetary shock waves—Evidence for magnetic bottles, J. Geophys. Res., 78, 2001–2009.

Gosling, J. T., D. N. Baker, S. J. Bame, W. C. Feldman, R. D. Zwickl, and E. J. Smith (1987), Bidirectional solar wind electron heat flux events, J. Geophys. Res., 92, 8519–8535.

Hozworth, R.H. Norville, K.W., Williamson, P.R. (1987). Solar flare perturbations in stratospheric current systems, Geophys. Res. Lett. 14 (8), 52-855.

Lepping, R. P., C.-C. Wu, and D. B. Berdichevsky (2005), Automatic identification of magnetic cloud-like regions at 1 AU: Occurrence rate and other properties, Ann. Geophys., 23, 2687-2704. SRef-ID: 1432-0576/ag/2005-23-2687

Maris O., Maris G (2005) Specific features of the high-speed plasma stream cycles. Advances in Space Research 35 (12), 2129-2140, doi:10.1016/j.asr.2005.02.068

Mavromichalaki, H., Vassilaki, A., Marmatsouri, E. (1988) A catalogue of high-speed solar-wind streams: Further evidence of their relationship to Ap-index. Solar Physics, Volume 115, Issue 2, pp.345-365, DOI:10.1007/BF00148733,

Mavromichalaki, H., Vassilaki, A. (1998) Fast Plasma Streams Recorded Near the Earth During 1985–1996. Solar Physics 183, 181–200. https://doi.org/10.1023/A:1005004328071

Richardson, I.G., Cane, H.V., Cliver, E.W. (2002) Sources of geomagnetic activity during nearly three solar cycles (1972-2000). JGR Space Physic 107 (A8), CiteID 1187, DOI 10.1029/2001JA000504,

Richardson, I. G., and H. V. Cane (2010), Near-Earth interplanetary coronal mass ejections during solar cycle 23 (1996–2009): Catalog and summary of properties, Sol. Phys., 264, 189.

Skoug, R. M., W. C. Feldman, J. T. Gosling, D. J. McComas, and C. W. Smith (2000), Solar wind electron characteristics inside and outside coronal mass ejections, J. Geophys. Res., 105, 23,069–23,084.

Tsurutani B.T.; Gonzalez, W. D. (1997), The Interplanetary causes of magnetic storms: A review. In: Magnetic Storms., Geophys. Monogr. Ser., vol. 98, edited by B. T. Tsurutani et al., pp. 77-89, AGU, Washington, D. C.

Venkatesan D., Shukla A.K., Agrawal S.P., (1982) Cosmic-Ray Intensity Variations and Two Types of High-Speed Solar Streams, Solar Physics 81 (2), 375-381,

Yermolaev, Y.I., Nikolaeva, N.S., Lodkina, I.G. et al. (2009). Catalog of large-scale solar wind phenomena during 1976–2000. Cosmic Res 47, 81–94, https://doi.org/10.1134/S0010952509020014

Xu F., Borovsky J.E. (2014) A new four-plasma categorization scheme for the solar wind, JGR Space Physics 120 (1) 70-100, https://doi.org/10.1002/2014JA020412